Heliyon 9 (2023) e18798

Contents lists available at ScienceDirect

Heliyon

journal homepage: www.cell.com/heliyon

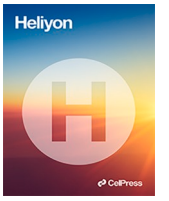

Formulation and characterization of cisplatin-loaded hydroxyl functionalized single-walled carbon nanotubes for targeting gastric cancer stem cells

A.N.K.V. Sravani, Natarajan Chandrasekaran *, John Thomas, Amitava Mukherjee

Centre for Nanobiotechnology, Vellore Institute of Technology (VIT), Vellore, 632014, Tamil Nadu, India

ARTICLE INFO

Keywords:
Cisplatin
Hydroxyl functionalized single-walled carbon nanotube
Gastric cancer stem cells
Stem cell markers
Tumorspheres

ABSTRACT

Chemotherapy is the most commonly used therapeutic method for treating many malignancies including gastric cancer. Due to their non-specific and non-targeted drug delivery, it causes resistance leading to cancer progression, relapse, and metastasis of cancer. To overcome this problem we carried out a study aimed to develop a new cisplatin (Cisp) loaded hydroxyl functionalized single-walled carbon nanotube (OH-SWCNT) nanocarrier system to selectively eliminate gastric cancer stem cells. To our understanding, this is the first study of the non-covalent interaction of cisplatin loaded on the surface of hydroxyl-functionalized single-walled carbon nanotubes by ultrasonication. The physical and morphological characterization was carried out by UV–Vis, FTIR spectroscopy, and TEM. A sustained and controlled release of cisp from OH-SWCNT at all three pHs 3.5, 5.5, and 7.4 was observed. Gastric cancer stem cells were isolated from primary cells and were identified by using $CD133^+$ and $CD44^+$ specific markers. Cisplatin-loaded OH-SWCNT nanocarrier was capable of limiting the self-renewal capacity of both $CD133^+$ and $CD44^+$ populations and also decreasing the number of tumorspheres in gastric CSCs. The cell viability percent of AGS cells was 20% at 250 μg/ml concentration. The IC50 value was less than 50% mol/L at both 200 μg/ml and 250 μg/ml of cisplatin-loaded OH-SWCNT. Our findings suggest that cisplatin-loaded OH-SWCNT nanocarrier complexes could target gastric CSCs and also could provide a potential strategy for selectively targeting and efficiently eliminating gastric CSCs. This could be a promising approach to prevent gastric cancer recurrence and metastasis and also improve gastric cancer therapy.

1. Introduction

Cancer is a life-threatening disease that causes mortality and morbidity in all age groups. Gastric cancer is the fourth most common cancer in the world and the second leading cause of cancer-related mortality [1,2]. There are around one million new instances of cancer illness every year, with 8.5 lakh fatalities [2]. Though much advancement has been made in medical science, a complete cure for gastric cancer is still in its infancy [2]. Although chemotherapy is a common method in gastric cancer treatment, the overall survival rate is 20%. This may be due to poor solubility of the drug, inactivation, and degradation, choice of drug, poor distribution, and difficulty in overcoming biological barriers and delivering a drug to the targeted site of action [3,4].

* Corresponding author.
E-mail addresses: nchandrasekaran@vit.ac.in, nchandra40@hotmail.com (N. Chandrasekaran).

https://doi.org/10.1016/j.heliyon.2023.e18798
Received 15 December 2022; Received in revised form 27 July 2023; Accepted 27 July 2023
Available online 2 August 2023

Recent studies have shown that some cells remain active post-chemotherapy and radiotherapy [5]. The remaining cells, which are resistant recover at the later stage of cell growth having stem-like properties and their functions are referred to as cancer stem cells (CSCs) [5,6]. Cancer stem cells (CSCs) are a class of pluripotent cells whose behavior is identical to normal stem cells having the ability to proliferate into a range of cell types as seen in many tumors [7–10]. Many clinical shreds of evidence show that the existence of CSCs comprises a significant fraction of the tumor mass in the tumor recurrence even after effective therapy and this contributes to tumor aggression. Chemotherapy and radiation can kill only differentiated cancer cells but not undifferentiated CSCs. These cells remain dormant, have the potential for intrinsic detoxification, and can hide in hypoxic niches or use other mechanisms to evade these therapies [11]. Currently, CSCs have emerged as new anti-cancer therapeutic targets. Developing CSCs-targeting therapeutics to remove CSCs has a significant clinical impact on cancer therapy.

The specific gastric cancer stem cell markers $CD133^+$ and $CD44^+$ are extensively used for identifying gastric cancer stem cells [12–16]. The $CD133^+$ cell surface marker is a Pentamembrane glycoprotein, which is identified in various cancer types, including colon and liver cancer [12]. Several studies have also shown that it is expressed even in gastric cancer [13,14]. The $CD133^{++}$rich cells have high self-renewal ability and tumorigenicity. The cell surface adhesion receptor $CD44^+$ which is involved in cell adhesion is abundant in many malignancies and is also frequently employed as a marker of gastric cancer stem cells [14]. It has a higher sphere-forming capacity *in vitro*, as well as migratory and invasive potential, drug resistance, and tumorigenic potential *in vivo* [17,18]. Although there are several studies on targeted treatment for cancer stem cells, they addressed only one population of cells with a particular marker. The present study however aims to target multiple populations of gastric cancer stem cells because gastric cancer stem cells possess multiple populations of cells with different cell-specific markers. Targeting cancer stem cells using nanoparticles may give better therapeutic effectiveness. In this study, we have chosen carbon nanotubes as a drug delivery vehicle because of their biocompatibility and biosafety.

Carbon nanotubes are versatile drug delivery carriers due to their unique chemical and physical properties and many appealing features such as the high length-to-diameter aspect ratio, mechanical strength, economical availability, biocompatibility, and environmental friendliness which make them very appropriate for a wide range of biomedical applications [19]. Among them, OH-SWCNT is a rolled-up single layer of graphite with long, tubular fullerene structures having a tube diameter of 0.4–2 nm with hexagonal carbon walls and pentagonal rings at its endpoints [20]. Hydroxyl functionalized single-walled carbon nanotubes can cross cell membranes which seems to be one of its special characteristic features suitable for targeted drug delivery [21,22]. The OH-SWCNT could finely hold drugs or other compounds which can be delivered to tumor sites *via* enhanced permeation and retention in a regulated manner, making them an ideal drug-loaded nanocarrier [23,24].

Cisplatin [*cis*-diamine platinum (II) dichloride] which was the first platinum-based drug approved by US FDA is a popular drug in cancer treatment [25]. Cisplatin works by inducing cytotoxicity and apoptosis in cancer cells. Even though cisplatin therapy is effective in many types of cancer, it causes severe nephrotoxicity in many cancer patients [26]. Cisplatin directly accumulates into cells and causes cytotoxicity, intracellular aquation, subcellular distribution, binding to cellular targets, and finally causing cellular damage that leads to cell death [27]. Cisplatin cellular accumulation is directly related to cytotoxicity, intracellular aquation, subcellular distribution, binding to cellular targets, and cellular damage that leads to cell death [27]. Besides that, drug resistance is one major issue caused by cisplatin treatment 10. This is due to Multi-drug resistance-associated proteins (MRPs) that alter drug transport within the cell by changing the glutathione system which eventually leads to treatment failure. To address the a forementioned issue, a targeted nanoparticle-based drug delivery system has emerged as a promising therapeutic strategy for overcoming cytotoxic toxicity and drug resistance. Hydroxyl functionalized single-walled carbon nanotubes have several potential applications in pharmaceutical products since it is non-toxic, biocompatible, and have physical properties.

In the present study, we formulated a CSCs targeting drug delivery system (OH-SWCNT-cisp) using hydroxyl functionalized single-walled carbon nanotubes (OH-SWCNTs) as drug carriers and cisplatin (Cisp) as the targeting ligand for the treatment of gastric CSCs. Using the high surface area of OH-SWCNT, cisplatin was loaded on them with a high drug-loading content *via* non-covalent interactions which also characterized both physically and chemically. The goal of our study was to formulate and characterize a pH-responsive cisplatin-loaded OH-SWCNT nanocarrier system to increase cisplatin efficiency, consisting of a controlled release profile, and also serve as an intracellular depot in acquiring chemosensitivity to assess the gastric CSCs-targeting.

2. Materials and methods

Hydroxyl functionalized single-walled carbon nanotubes (OH-SWCNTs) (quality level = 100) were purchased from Sisco Laboratories India, and Cisplatin (90.0% pure), insulin recombinant (90% purity) were purchased from Sigma Aldrich, United States. Tween80 (99.0% purity), Doublecons phosphate-buffered saline (DPBS, pH 7.0), Dulbecco's modified Eagle medium (DMEM), trypsin-EDTA, Penicillin- Streptomycin (Pen-Strep), fetal bovine serum (FBS), and EZcountTM MTT assay kit and EZcountTM WST-1 assay kit were purchased from Himedia labs Pvt ltd India. The AGS-CRL-1739 cell lines were obtained from the National Center for Cell Science and cell repository (NCCS), a non-profit organization concerning ATCC, Pune, India.

2.1. : Preparation of tween 80 dispersed OH-SWCNT

The hydroxyl functionalized single-walled carbon nanotubes (OH-SWCNT) 5 mg (w/v) were dispersed in 100 ml of 1.5% tween 80 surfactants and subjected to probe ultra-sonication. (Sonics, USA) for 30 min [28]. To mitigate the heat effect, sonication was carried out in cold conditions with 50 s on the pulse, 15 s off the pulses, and 40% amplitude. Then, the homogenous OH-SWCNT solution was transferred into 50 ml round-bottomed centrifuge tubes and centrifuged at 3000 rpm for 15 min to remove undispersed OH-SWCNT

After sonication, the preparation was centrifuged at 20 k rpm for 1 h and the well-dispersed OH-SWCNT was collected in supernatants. The sample was stored at 4 °C. Further, the dispersed OH-SWCNT was characterized by FT-IR and UV–vis absorption spectrophotometry.

2.2. : Loading of cisplatin onto the surface of OH-SWCNT

For the loading of cisplatin onto OH-SWCNT, each hydroxyl functionalized OH-SWCNT sample was reacted with the appropriate concentration of cisplatin (50,100, 150, 200, and 250 g/ml). This reaction was carried out by placing 2.5 ml of OH-SWCNT in a 10 ml vial by gradually adding 50 g/ml of cisplatin into the solution using a Pasteur pipette. The procedure was repeated for other cisplatin concentrations (100, 150, 200, and 250 μg/ml). The solutions were sonicated for 3 h in an ultrasonic bath and centrifuged at 3500 rpm for 5 min. Finally, the supernatant was collected and filtered using 0.45 μm pore size filters to remove undispersed drug bounds [29].

2.2.1. Characterisation of OH-SWCNT and cisplatin-loaded OH-SWCNT nanocarrier

FTIR of all three OH-SWCNT, cisp, and cisplatin-loaded hydroxyl functionalized carbon nanotubes (OH-SWCNT-cisp) were compared before and after non-covalent modification at each phase by using the KBR pellet method [3]. Briefly, fA 13 mm potassium bromide (KBr) powder was mixed and ground thoroughly using a mortar and pestle with the OH-SWCNT, cisp, and cisplatin-loaded hydroxyl functionalized carbon nanotubes (OH-SWCNT-cisp). The sample was placed in a pellet dye just sufficient enough to cover its bottom. It was pressed at 5000–10,000 psi using the pellet press to form a pellet disc and placed in the sample holder It was then analyzed by FTIR (Jasco 6800) of each compound spectrum with a resolution of 4 cm-1 spanning the wavenumber range of 399–4000 cm-1. The morphology of cisplatin-loaded OH-SWCNT after modifications was examined using high-resolution transmission electron microscopy (HR-TEM) (FEI –TECNAI G2-20 TWIN of China (Operating voltages 200 kV). The dispersed samples were drop-coated onto a Cu grid and dried at 55 °C before observation.

2.3. Drug entrapment and in-vitro drug release kinetics

The drug entrapment efficiency involves the determination of the quantity/amount of cisplatin loading onto OH-SWCNT. This procedure was carried out by a UV–Visible spectrophotometer. First, the standard calibration curve of cisplatin was plotted by diluting a stock solution of cisplatin of various concentrations like 50,100,150,200, and 250 μg/ml by taking 0.5 ml solution with 4.5 ml of double distilled water and measuring the absorbance at λ max 237 nm in UV–Vis spectrophotometer [29]. The drug entrapment efficiency (EE) was calculated using the following equation 1

$$Entrapment\ Efficency = \frac{The\ weight\ of\ drug\ entraped\ on\ OH-SWCNT}{Weight\ of\ drug\ intially\ loaded} \times 100 \quad (1)$$

The *in-vitro* release of cisplatin-loaded OH-SWCNT at two endosomal pHs 7.4 and 5.5 3.5 was evaluated by the dialysis tubing cellulose membrane method. Briefly, the cisplatin-loaded OH-SWCNT nanocarrier was placed into a dialysis membrane with an average flat diameter of 10 mm (millimeter) and molecular weight of 10,000 kDa, with a capacity of 10 ml (w/v). Further dialysis of the cisplatin-loaded OH-SWCNT was done individually by submerging the bag in 50 ml of 1× simulated gastrointestinal fluid with pHs of 3.5, 5.5, and 7.4. The solution was covered with thin Parafilm to minimize evaporation and continuously stirred using a magnetic stirrer for 150 rpm maintaining the temperature at 37 °C. To maintain a constant volume of 3 ml OH-SWCNT-cisp samples from the gastrointestinal fluid were removed and substituted with the same 3 ml of fresh medium at fixed time intervals respectively [30]. The quantity of drug in each sample was determined using UV–visible spectroscopy at λmax of 237 nm (cisp) their standard values. The following equation (2) was used to express cumulative drug release percent about time [30].

$$Cumilativedrugrelease(\%) = \frac{Amount\ of\ drug\ released}{Total\ drug\ loaded} \times 100 \quad (2)$$

2.4. Cell culture

The HEK and AGS cell lines were cultured in a DMEM medium containing 10% fetal bovine serum and 1% penicillin-streptomycin in T25 cm^2 flasks. The flasks were incubated at 37 °C in a humidified environment with 5% CO2 to facilitate the monolayer formation [31]. Depending on the cell type, the cell culture medium was changed every two to three days, and the cells were checked for growth and contamination regularly. When the cells attained 80% confluency the cells were trypsinized with 2% trypsin EDTA.

2.5. MTT assay

MTT assay was used to study the cell viability of the synthesized sample [32]. The cells were stained with trypan blue and counted using a hemocytometer. Further, 4×10^3 cells were seeded onto the well plate and incubated overnight at 37 °C with 5% CO_2 [31]. After achieving 80% confluence, the cells were treated with various concentrations of all three samples of OH-SWCNT, cisplatin, and cisplatin-loaded OH-SWCNT nanocarrier in (50–250 μg/ml) for 3 h. MTT solution (20 μl/ml) was added to each well and incubated for 3 h s. The supernatant was discarded and 100Ml of DMSO was added to each well and incubated for 1 h at 37°c. The cell viability was observed using an ELISA plate reader (Bio-Rad) at 570 nm. The percentage of cell viability was calculated using the following equation

(3) and the values were represented as mean standard deviation (SD) (n = 3). The IC50 values were calculated individually for all HEK and AGS cell lines.

$$\text{Cell viability } \% = \frac{Absorbance\ of\ treated}{Absorbance\ of\ control} \times 100 \quad (3)$$

2.6. Isolation, identification, and culturing of gastric CSCs

2.6.1. Spheroid formation assay

Human gastric cancer stem cells (AGS CSCs) were isolated from AGS cells (National Center for cell sciences and cell repository: Pune) when they reached 70–80% confluency and then a single-cell suspension of 1×10^6 cells/ml was prepared *via* digestion using 0.25% trypsin-EDTA. The isolated gastric cancer CSCs were cultured in 6 well ultra-low attachment plates (Corning Life Sciences, Acton) and are supplied with 2–3 ml of serum-free Dulbecco's modified Eagle's medium supplemented supplying 5% CO_2 at 37 °C. After 2 weeks, each well was examined using a fluorescence inverted light microscope, and the total no of spheroid colonies was counted. Images of the spheroid colonies were recorded using light and fluorescence dual microscopy (ZEISS Axio Vert.A1).

2.7. Flow cytometer analysis and fluorescence-activated cell sorting

For surface marker analysis by flow cytometer, 70%–90% confluent cells were washed once with phosphate-buffered saline, and cells were then dissociated from plates using Trypsin-EDTA, further centrifuged and re-suspended with 5×10^6 cells per well in 6-well ultralow attachment plates. They were then washed with 2% FACS buffer (1 ml PBS containing 2%FBS). The cells were then stained with 10 μg/ml primary anti-CD133 and CD44 antibodies (dilutions made with FACS buffer if required) and incubated at 4 °C for 30 min. The samples were then washed three times with cold PBS (pH 7.4) and re-suspended in FACS buffer (PBS with 2% FBS) for flow cytometer analysis [12]. The results were analyzed with a flow cytometer (Cytoplex Flow cytometry; Beckman Coulter). Side scatter and forward scatter profiles were used to eliminate cell doublets.

2.7.1. Culturing of CD133 and CD44 cell surface marker-specific stem cells

For the culture of marker-specific gastric CSCs, the $CD133^+$and the $CD44^+$fractions from the FACS sorted AGS CSCs were seeded in a 6-well ultralow attachment plate (Corning, Lowell, MA, USA) and cultured in stem cell medium, i.e. DMEM medium supplemented with recombinant insulin and 100 μg/ml penicillin, and 100 mg/ml streptomycin in a humidified incubator with 5% CO2 at 37 °C. Under these conditions, the AGS CSCs grow as non-adherent spherical clusters of cells and tumor spheres. Tumrospheres were collected by centrifugation at 1000 rpm for 5 min and further plated at 1×10^4 cells/ml in the same medium for future experiments.

2.8. Self-renewal capacity inhibition assay of gastric CSCs

2.8.1. $CD133^+$ and $CD44^+$ proliferation inhibition assay

$CD133^+$ and $CD44^+$ specific stem cells were suspended in DMEM medium and seeded onto a 6-well ultralow attachment culture plate. 5×10^5 cells/well were cultured in the well plate in a humidified atmosphere of 5% CO_2 at 37 °C for 24 h. Then, three different samples namely free OH-SWCNT, and cisplatin-loaded OH-SWCNT are diluted with 1 ml of the complete medium at concentrations of 50,100,150,200 and 250 μg/ml were added to a 6-well ultra-low attachment plate and incubated for 48 h [12]. The blank culture medium was used as a control. After 48 h of treatment, the cells were harvested, washed, and suspended at a density of 2×10^6 cells/mL in medium (DMEM medium containing 2% FBS), then the $CD133^+$ and $CD44^+$ marker-specific stem cells were analyzed for their antiproliferative activity using WST-1 kit assay through reading the absorbance on a microplate reader (BIO-RAD model 680, Bio-Rad Laboratories, Inc. Shanghai, China) at the wavelength of 450 nm [33]. The survival rate was calculated from the following equation (4). The dose effect for both $CD133^+$ and $CD44^+$ is calculated in duplicates (n = 2).

$$\text{Survival } \% = \frac{A450nm\ for\ the\ treated\ cells}{A450nm\ for\ the\ control\ cells} \times 100 \quad (4)$$

2.8.2. Tumrosphere formation inhibition assay

The inhibitory effect of tumrosphere formation in both $CD133^+$ and $CD44^+$ cells following treatment with various concentrations of cisplatin-loaded OH-SWCNT was measured using the tumrosphere assay method [1]. Briefly, $CD133^+$ and $CD44^+$ cells with a good density of 3×10^5 cells/well were seeded in 6-well ultralow attachment plates and supplemented with DMEM medium containing 5% FBS, 100 U/mL penicillin, and 100 mg/ml streptomycin. After 24 h the cells were treated with free OH-SWCNT and OH-SWCNT-cisp at various concentrations like 50 μg/ml,150 μg/ml, and 250 μg/ml (according to IC_{50} value) were added respectively [12]. Here, PBS acted as a blank or control. These cultures were maintained at 37 °C with a 5% CO2 atmosphere for 7 days. The tumrosphere formation was observed and photographed using an inverted fluorescence microscope (ZESSIS AXIOV1 edition).

3. Results and discussion

3.1. Formulation and characterization of OH-SWCNT and cisplatin-loaded OH-SWCNT nanocarrier

The procured OH-SWCNT was homogeneously dissolved in 1.5% of Tween80 solution employing the ultra-sonication method as shown in Fig. 1(A). The experimental results revealed that after centrifugation, there was no visible precipitation or sedimentation. The UV–visible spectra of OH- SWCNT were measured at a wavelength range of 200–800 nm. The plasmon resonance peak was observed at 252 nm corresponding to 4.88eV as shown in Fig. 1(C). As, OH-SWCNT are hollow tubular structures they have high van der Waals force of interactions, and hydrophobic properties, which tend them to form agglomerates in aqueous solution with any non-ionic surfactants [19]. The underlying mechanism is the hydrophobicity nature of the tails of Tween 80 getting adsorbed onto the surface of OH-SWCNT and the hydrophilic heads facing towards the aqueous phase, by lowering the interfacial tension. Hence our experimental results were found are agreed with the findings of Haruhisa Kato et al. [33] and Markovic et al. [34].

Due to the three-dimensional nature of cisplatin, the aromatic rings of cisplatin are not in a plane and therefore there is no stable non-covalent interaction between cisplatin and carbon nanotubes [35]. To overcome this we used ultra-sonication to load cisplatin onto the surface of OH-SWCNT by creating non-covalent interactions. Our experimental results revealed that successful loading cisplatin at various concentrations (50μg/ml-250 μg/ml) was observed under UV–visible spectra showing an absorbance peak at λmax of 237 nm as shown in Fig. 1(D). No visual sedimentation was observed on centrifugation as shown in 1(B). The loading efficiency of cisp on OH-SWCNT was increased upon the increase in the concentration of cisplatin loaded as shown in Fig. 1(D).

FTIR spectra of all three samples namely OH-SWCNT, cisp, and cisplatin-loaded OH-SWCNT are shown in Fig. 2(A). The OH-SWCNT showed a broad spectrum at 3566.7 cm^{-1} which indicates the presence of the –OH group of OH-SWCNT. The peak at 3339.14 cm^{-1} could be attributed is due to the stretching vibration of water molecules. In cisplatin, characteristic peaks observed at 1621.84 cm^{-1} and 2106.84 cm^{-1} are due to strong C–H bending vibration and strong N═C═S stretching vibrations of aromatic compounds. The FTIR data of cisplatin loaded OH-SWCNT-nanocarrier show peaks at 2353.69 cm^{-1} and 1627.51 cm^{-1} which are

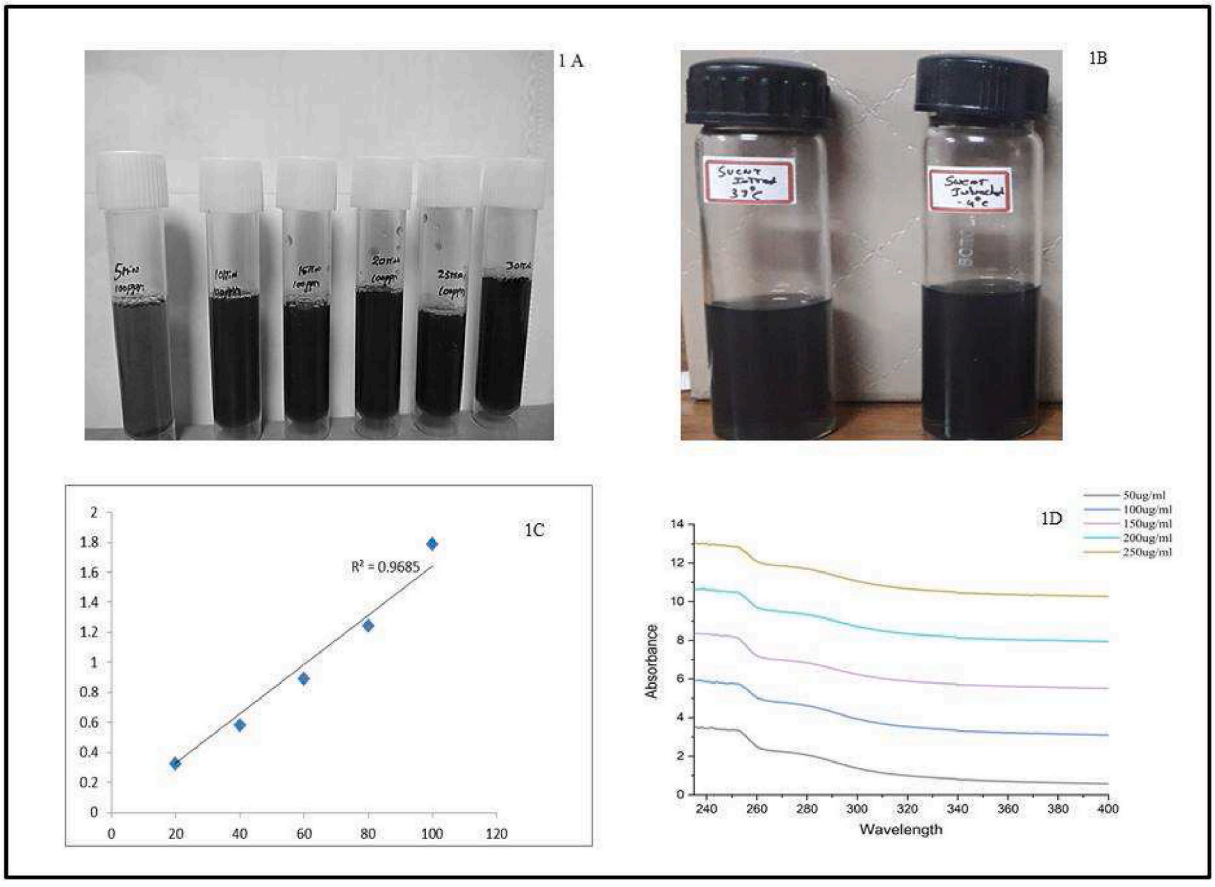

Fig. 1. 1A) Uniformly dispersed Hydroxyl functionalized Single-Walled carbon nanotubes in 1.5% tween 80 solutions at various time limits.1B) Homogeneously dispersed cisplatin in OH-SWCNT and is stable at both room temperature and -4°c on centrifugation. 1C) Linear plot derived from UV–visible data for Hydroxyl functionalized Single-walled carbon nanotubes at 252 nm. 1D) UV–visible spectra of loading efficiency of cisp onto OH-SWCNT surface at various concentrations (50–250 μg/ml) at λmax 237 nm.

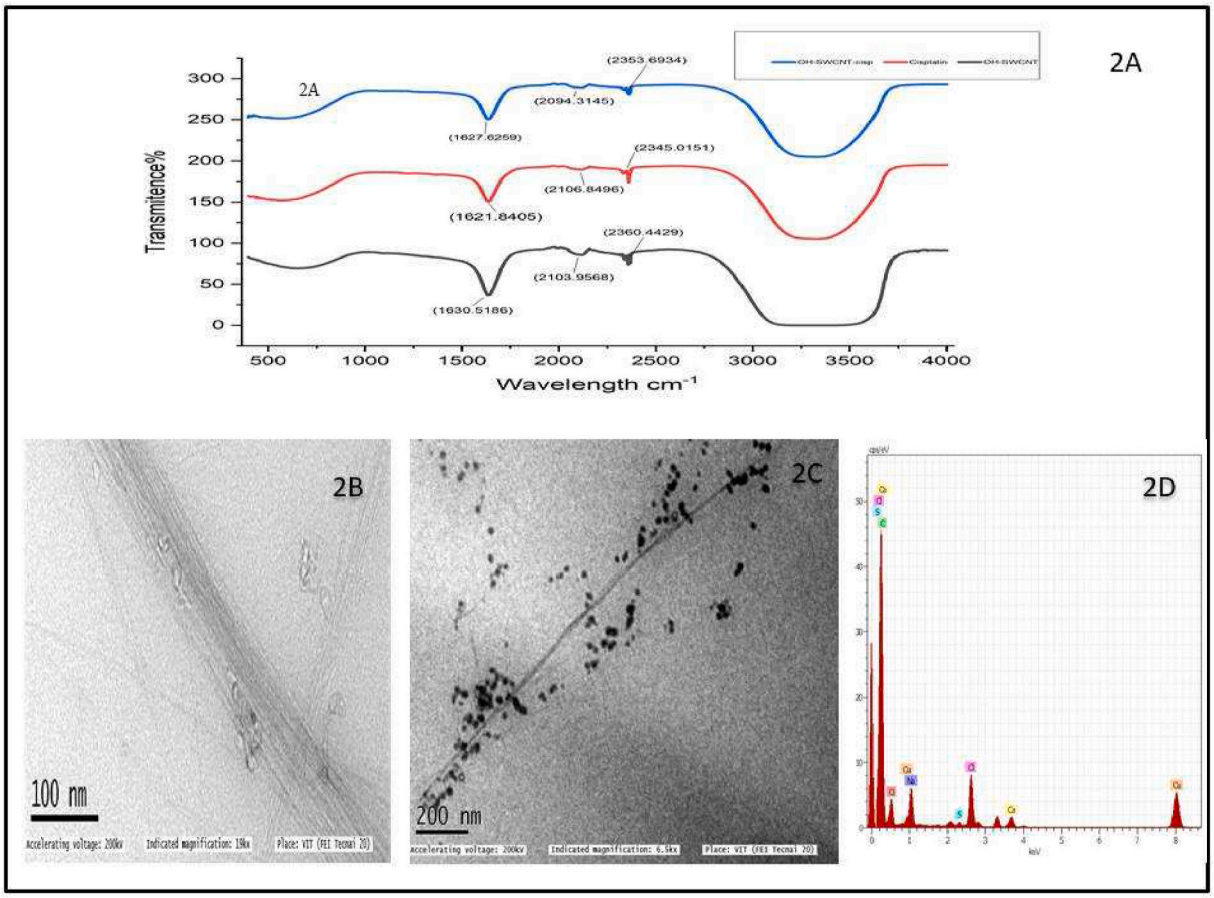

Fig. 2. 2(A) FTIR spectra of OH-SWCNT, cisplatin, and cisplatin-loaded OH-SWCNT. 2(B) TEM image of tween 80 surfactants dispersed OH-SWCNT with a size diameter of 100 nm; 2(C) TEM image of cisplatin loaded OH-SWCNT nanocarrier with a size diameter of 200 nm; 2(D)EDX of cisplatin-loaded OH-SWCNT.

slightly upshifted and also peaks which were downshifted to 2094.48 cm^{-1} when compared to FTIR data of OH-SWCNT indicating cisplatin non-covalently interacted with OH-SWCNT.

The surface morphology of cisplatin-loaded OH-SWCNT and EDX are shown in Fig. 2(B). The size of OH-SWCNT–cisp with a tube diameter was measured and found to be 150 nm long. The cisplatin showed a scattered distribution pattern on the exterior surface of OH-SWCNT as in Fig. 2(B). This explains that the lattice fringes of carbon walls have interacted non-covalently with cisplatin on its surface. We believe this interaction could be one of the crucial elements in our study which shows the impact upon loading, delivery, and release kinetics of cisplatin-loaded OH-SWCNT nanocarrier. Our experimental data was similar to the findings by Shuoye Yang et al. who reported the noncovalent conjugation of carboxylated SWCNTs which with PEG groups after acidification formed a tubular structure of CNTs-PEG and CNTs-PEG-PEI nanoconjugates. They reported that these CNTs-PEG-PEI nanoconjugates are rough in appearance and some of their particles appear to be attached and distributed along the sidewalls of CNTs which indicate dual non-covalent conjugation of both PEG and PEI onto carbon nanotubes [30].

Table 1
Drug entrapment efficiency of cisplatin–loaded OH-SWCNT nanocarrier at different concentrations (50μg/ml-250 μg/ml) on UV–visible data. The highest entrapment efficiency is found at 200 μg/ml.

OH-SWCNT –cisp	Entrapment Efficiency
OH-SWCNT-cisp (X50 μg/ml)	54.7%
OH-SWCNT-cisp (X100 μg/ml)	89.99%
OH-SWCNT-cisp (X150 μg/ml)	93.56%
OH-SWCNT-cisp (X200 μg/ml)	95.82%
OH-SWCNT- cisp (X250 μg/ml)	81.86%

3.2. Drug entrapment efficiency and release kinetics of cisplatin-loaded OH-SWCNT nanocarrier

Drug entrapment efficiency is one of the crucial factors for developing an effective drug delivery carrier system. The OH-SWCNT nanocarriers have 91% of drug-loading ability [36] which made us choose OH-SWCNT for loading cisplatin in our study. OH-SWCNT in our study was chosen to be an effective drug carrier. The encapsulation efficiency of cisplatin loaded on the surface of OH-SWCNT was observed for different concentrations like 50 μg/ml, 100 μg/ml, 150 μg/ml, 200 μg/ml, and 250 μg/ml which showed the highest entrapment efficiency to be 95% at 200 μg/ml at 237 nm is as shown in Table 1.

The drug release rate and overall time are crucial factors for studying the cumulative release kinetics of a drug. Therefore the cumulative drug release response of cisplatin for our formulation was carried at two different physiological pHs (3.5, 5.5, and 7.4) in simulated gastrointestinal fluid with a varying time of 48 h. Results are shown in Fig. 3. The experimental results showed that at pHs 3.5 and 5.5 the release percent of cisplatin was faster than the release percentage at pH 7.4 in the first 6 h. This may be due to the unbounded cisplatin on the surface of OH-SWCNTs. Within 48 h of investigation, the release percentage of cisplatin was 69% at pH 3.5, 68% at pH 5.5, and 72% at PH 7.4. This may be due to the non-covalent interaction of cisplatin with OH-SWCNT nanoparticles which would get detached easily in acidic pHs (3.5 and 5.5). The mechanism behind this is an exchange of anions and transfer of a proton (protonated reaction) facilitating detachment from OH-SWCNT [36]. There was also a long-term release observed throughout 48 h at all pHs (3.5, 5.5 &7.4). This might be due to the Half-life of cisp loaded on OH-SWCNT being more than 48 h which facilitates the release of cisplatin in a controlled and sustained manner from the exterior surface of OH-SWCNT [37]. It is also observed not much difference in release data at pH 3.5 when compared to pH 5.5 at all 48 h of release. Therefore, the release of cisplatin over OH-SWCNT was pH-dependent and pHs 3.5 and 5.5 was chosen as the suitable pHs for the release of cisplatin over the surface of OH-SWCNT because of the acidic environment which is suitable for better stimulation of drug delivery to the tumor site *via* the gastric region. Hence, our results show that cisplatin-loaded OH-SWCNT is a potential anticancer drug delivery nanocarrier for targeting tumor cells.

3.3. In-vitro cytotoxicity of cisplatin-loaded OH-SWCNT nanocarrier

In-vitro cytotoxicity studies on normal Human kidney cell lines (HEK) and Human gastric cancer cell lines (AGS) were carried out using the MTT assay method to check the pharmacological activity of cisplatin-loaded OH-SWCNT. Fig. 4 (A&B) shows the cell viability percentage of both HEK and AGS cells that were subjected to different concentrations of OH-SWCNT, cisplatin, and cisplatin-loaded OH-SWCNT ranging from (50–250 μg/ml) respectively. Our results showed that the cell viability percent of cisplatin-loaded OH-SWCNT and cisplatin have the least viability percentage and are toxic to cancer cells upon an increase in their concentration. Whereas, in comparison to cisplatin-loaded OH-SWCNT, OH-SWCNTs exhibited the least cytotoxicity at all concentrations. As OH-SWCNT showed no significant difference in the viability of AGS cells the cytotoxicity caused may be due to cisplatin only. All the values are calculated in duplicates and the results obtained were statistically significant with a $p\text{-value} < 0.05$ when determined with TWO-way ANOVA. The IC_{50} values for cisplatin-loaded OH-SWCNT at all concentrations (50–250 μg/ml) were calculated and summarized in Table 2. The IC_{50} of cisplatin-loaded OH-SWCNT was 25.785 ± 1.754 (mol/L) at 250 μg/ml. We also performed a cytotoxicity assay on normal HEK cell lines to evaluate the selectivity of the drug-loaded nanocarrier system. Having into consideration that when we performed an MTT assay on HEK cells we observed poor cytotoxicity where our results correlate to the study reported by

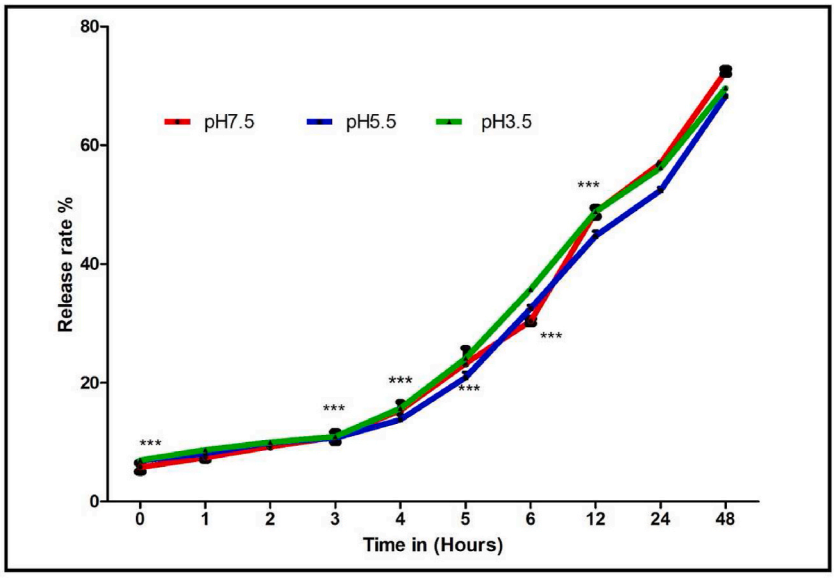

Fig. 3. Cumulative drug release kinetics of cisplatin from OH-SWCNT in simulated gastrointestinal fluid at pHs (3.5,5.5 and 7.4) at 37 °C room temperature. Data represent the mean ± SD (n = 2) with *P-Value* < *0.05*.

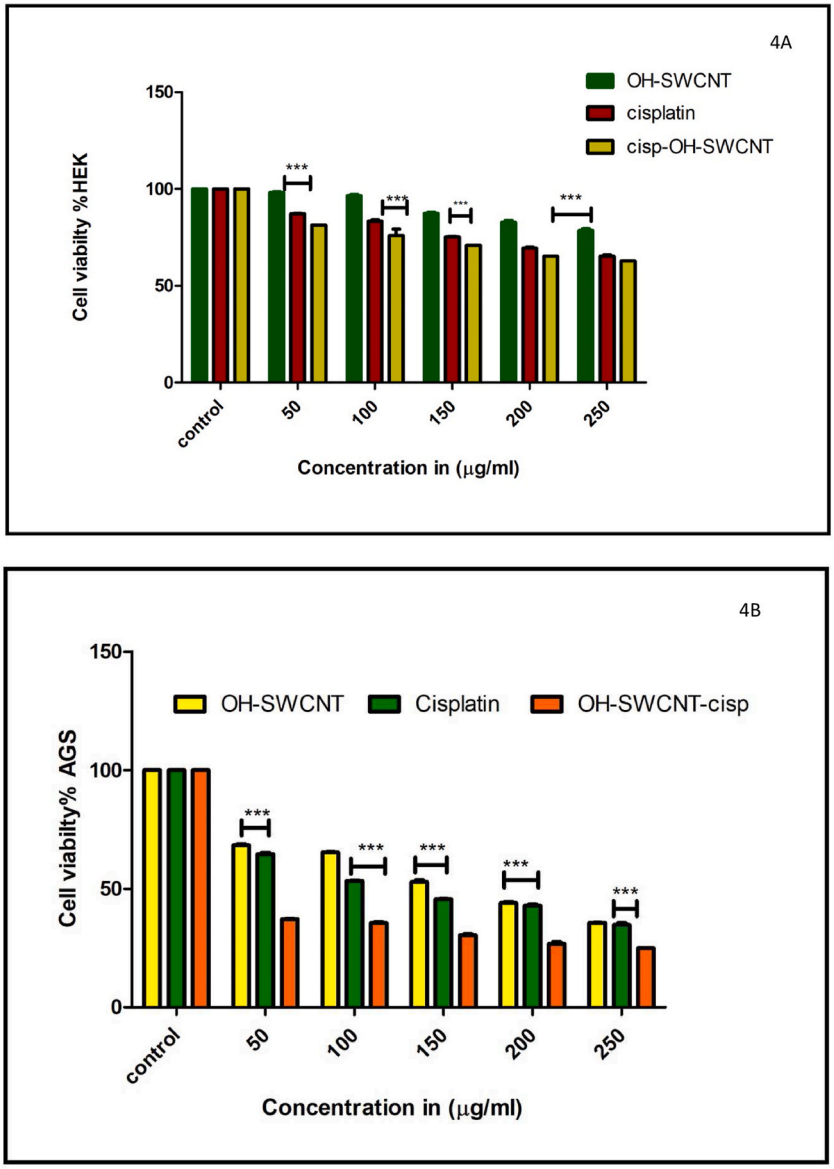

Fig. 4. 4(A) Concentration-based cell viability percent of OH-SWCNT, cisplatin, and cisplatin-loaded OH-SWCNT in HEK cell lines.MTT test was used to determine the number of cells (as a percentage of control). 4(B)Concentration-based cell viability percent of OH-SWCNT, cisplatin, and cisplatin-loaded OH-SWCNT in AGS cell lines.MTT test was used to determine the number of cells (as a percentage of control). The error bar depicts the standard deviation (n = 2) *** is used to indicate *P-values* < 0.001–0.005.cells.

Table 2
Calculated IC_{50} from the 4 PL fitted curve for OH-SWCNT, cisplatin, and cisplatin loaded OH-SWCNT nanocarrier in AGS cell lines with the comparison of HEK cell lines with 95% confidence intervals.

Cell lines	OH-SWCNT Mean ± SEM (mol/L)	Cisplatin Mean ± SEM (mol/L)	Cisplatin loaded OH-SWCNT Mean ± SEM (mol/L)
AGS	56.86 ± 5.566	45.925 ± 2.589	25.785 ± 1.754
HEK	143.61 ± 3.861	56.02 ± 7.213	78.92 ± 4.136

O.O. Ogbole et al. [38]. Our results say that there is not much cytotoxicity in HEK cells even at a higher concentration of 250 μg/ml. All the values are calculated in duplicates and the results obtained were statistically significant with Two–way ANOVA showing no significant difference with a *p-value* > 0.05. The calculated IC_{50} obtained for biocompatibility of nanocarrier-based drug delivery in the normal HEK cell lines was 56.02 ± 7.213 mol/L (cisp), 143.61 ± 3.861 mol/L (OH-SWCNT), and 78.92 ± 4.136 mol/L

(cisp–OH–SWCNT) which represents negligible toxicity in the case of nanocarrier system like cisp loaded OH-SWCNT when compared to IC_{50} of cisplatin probing for their biocompatibility for other nanomedicine applications.

3.3.1. Isolation, identification, and culturing of $CD133^+$ and $CD44^+$ gastric cancer stem cells

Cancer stem cells are believed to be able to form spheres in a culture that are similar to endogenous cancer cells [35,39]. Therefore, we cultured gastric cancer stem cells in a serum-free medium for forming spheres as shown in Fig. 5(A). Further, we examined the sphere by using cell surface markers $CD133^+$, and $CD44^+$ using Fluorescence-activated cell sorting as shown in Fig. 5(B and C). The results showed that the percentages of gastric CSCs expressed with ($CD133^+$) specific cells were found to be 40.985 ± 0.0195 (mean ± SD) as shown in Fig. 5(B) and 32.185 ± 0.0138 for ($CD44^+$) specific cells out of the total CSC cells in the AGS cell line as shown in Fig. 5 (C).

The isolated $CD133^+$ and $CD44^+$ CSCs from AGS cell lines were cultured in a serum-free medium for 3–4 weeks under non-adherent conditions to observe the self-renewal ability of gastric cancer stem cells. The results revealed that both $CD133^+$ and $CD44^+$ cells formed spheres having CSCs-like properties as shown in Fig. 5(D and E). We also developed secondary tumrospheres and maintained cultures for 12 passages by enzymatically dissociating the primary tumrospheres indicating that spheres of gastric CSCs have self-renewal capacity.

3.3.2. Proliferation inhibition assay

The proliferation inhibitory effect of OH-SWCNT, cisplatin, and cisplatin-loaded OH-SWCNT was observed on both $CD133^+$ and $CD44^+$ gastric CSCs as shown in Fig. 6. From our results, we observed that cisplatin showed chemo-resistance when treated at different concentrations (50 μg/ml-250 μg/ml) on treatment for 48 h and concluded that cisplatin has a critical role in determining the potential induction of chemo-resistance. However, when treated with Cisplatin loaded OH-SWCNT at various concentrations like (50–250 μg/ml) showed a stronger inhibitory effect on $CD133^+$ cells as shown in Fig. 6(A). This may be due to the accumulation of the highest intracellular platinum concentration of cisplatin on the surface of OH-SWCNT in Cisp-loaded OH-SWCNT which significantly improved

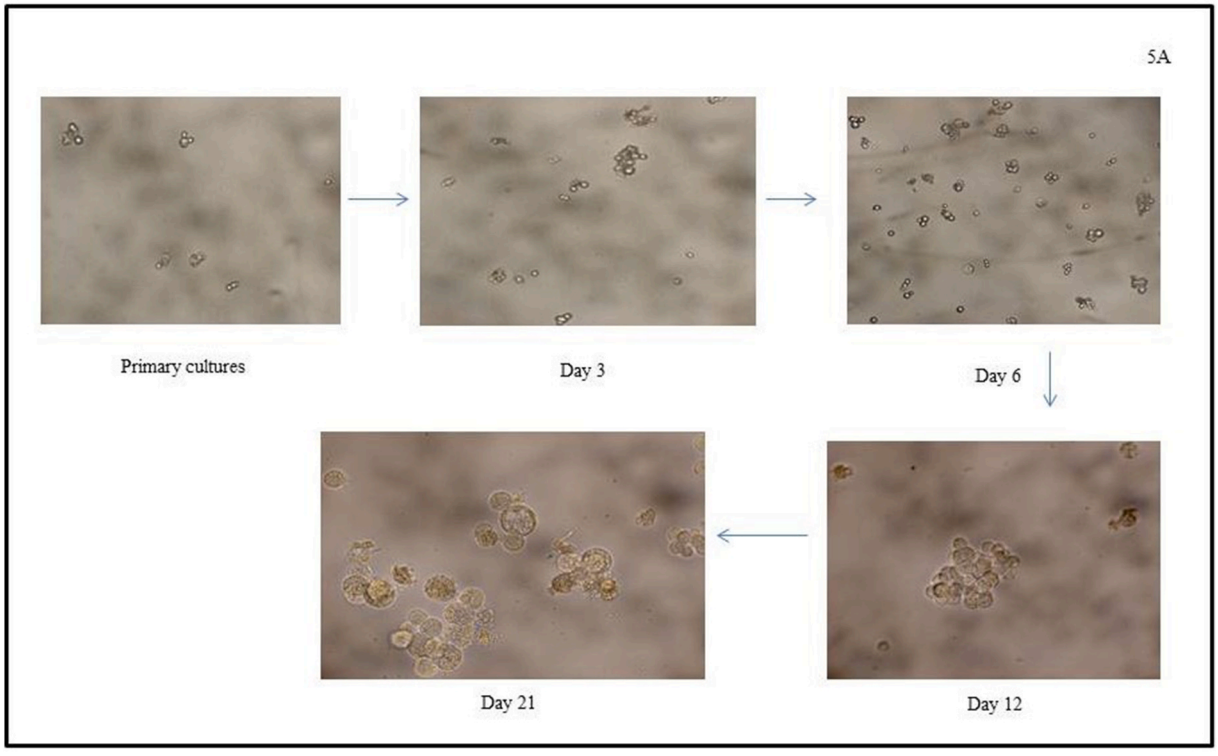

Fig. 5. 5(A) Human gastric CSCs cultures cultured from AGS cell line. Images explain the gradual increase in the number of gastric cancer stem cells from 3 to 21 days of culturing. (B) Expression of $CD133^+$ marker from gastric cancer lines AGS by fluorescence-activated cell sorting (FACS) analysis in comparison with control cells. Graphical representation of Positive average no $CD133^+$ spheroids formed on fluorescence-activated cell sorting is also shown in 5B, (C) Expression of $CD44^+$ marker from gastric cancer lines AGS by fluorescence-activated cell sorting (FACS) analysis in comparison with control cells. Positive Average no $CD44^+$ spheroids formed on fluorescence-activated cell sorting are also represented in the graph in Fig. 5B. From the graphical representation of both Fig. 5B and C the CD 133+ cells produced significantly higher numbers of spheroid colonies when compared to $CD44^+$ cells with a significant value of (p *value* < 0.01) (D) secondary spheroids colony formation of gastric cancer cell lines in serum-free media at 3–4 weeks of culture stained with anti-$CD133^+$-FITC antibodies, (E) secondary spheroid colony formation of gastric cancer cell lines in serum-free media at 3–4 weeks of culture stained with anti-$CD44^+$ FITC antibodies.

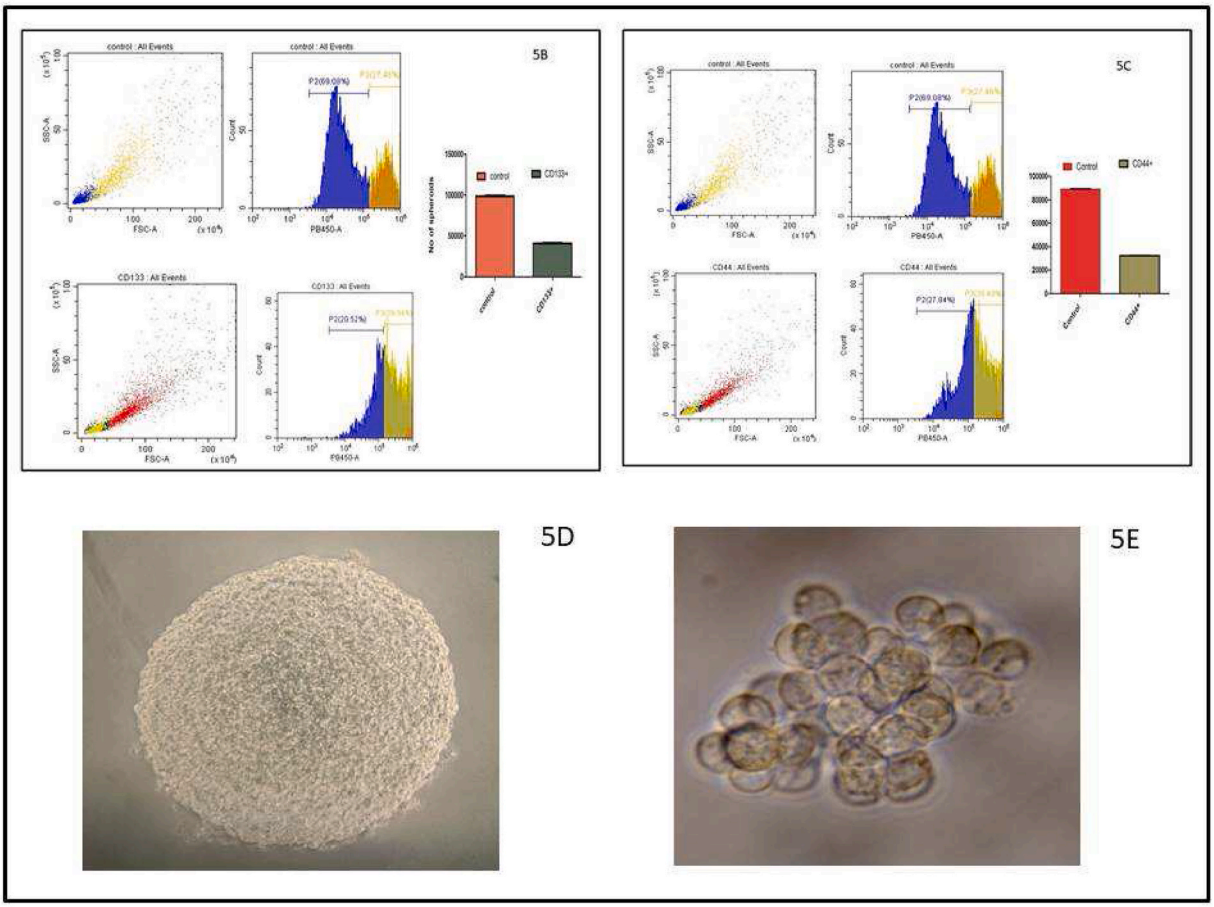

Fig. 5. (*continued*).

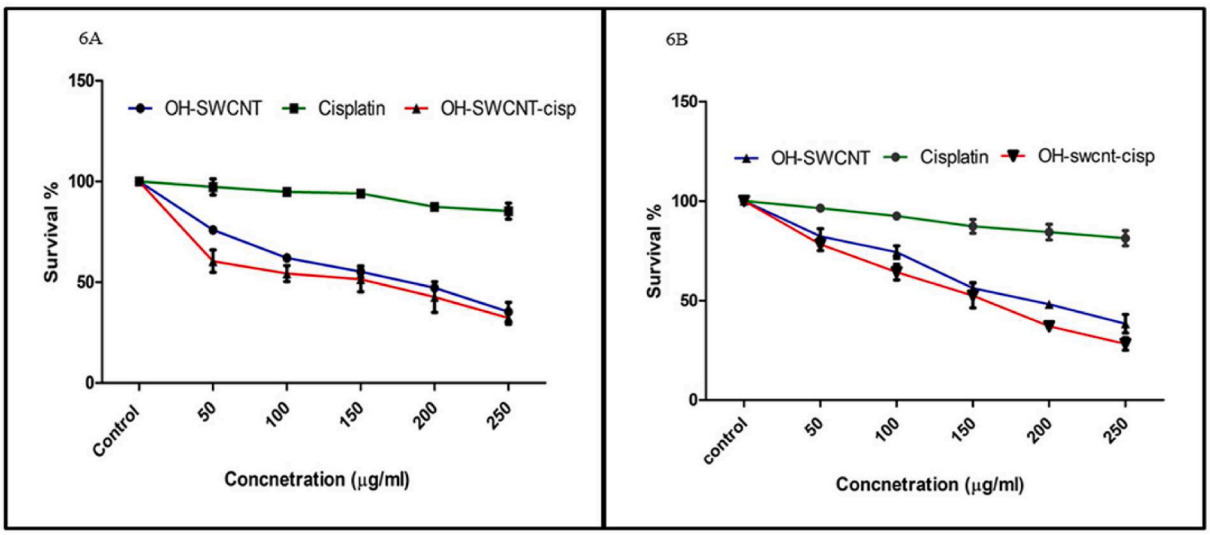

Fig. 6. Inhibitory effects to $CD133^+$ and $CD44^+$ gastric cancer stem cells 6(A) Inhibitory toxicity effect of cisplatin-loaded OH-SWCNT and OH-SWCNT on $CD133^+$ gastric cancer stem cells after applying various formulations at 48 h measured by WST-1 assay. Data are presented as the mean ± SD from duplicate (n = 2) experiments. $P < 0.001$. 6(B) Inhibitory toxicity effect of cisplatin, cisplatin loaded OH-SWCNT and OH-SWCNT on $CD44^+$ gastric cancer stem cells after applying various formulations at 48 h measured by WST-1 assay. Data are presented as the mean ± SD from duplicate (n = 2) experiments. ($P < 0.001$)' *** is used to indicate *P-values* < *0.001*.cells.

chemoresistance activity on its treatment either by direct and rapid partition of cisplatin into cell membrane. The inhibition profile of OH-SWCNT also showed that it does not have much inhibition effect which suggests that OH-SWNTs can be used as a CSCs-targeting vector for delivering anticancer drugs in CSC therapy. Whereas, similar results are also observed in $CD44^+$ cells upon 48 h of incubation as shown in Fig. 6(B). Cisplatin–OH–SWCNT significantly increased drug cytotoxicity in AGS CSCs, with a 7.6-fold decrease in CD133+ cells and a 4.9-fold decrease in $CD44^+$ cells in IC50 value compared to free cisplatin as shown in Table 3.

The percentage of cisplatin-loaded OH-SWCNT nanocarrier inhibiting proliferation capacity in both $CD133^+$ and $CD44^+$ tumorspheres was calculated as mean ± SD at all concentrations ranging from (50–250 μg/ml). It was observed that at 250 μg/ml concentration of cisplatin–loaded OH-SWCNT had the least survival percent of AGS CSCs. The survival percent rate of OH-SWCNT in $CD133^+$ CSCs at different concentrations (50–250 μg/ml) were to be 76.05 ± 0.138 (50 μg/ml), 62.04 ± 0.11 (100 μg/ml), 55.225 ± 0.619 (150 μg/ml), 47.16 ± 0.44 (200 μg/ml), 35.315 ± 0.867 (250 μg/ml) and Survival rate percent of cisplatin loaded OH-SWCNT in CD133+ cells 60.435 ± 1.197 (50 μg/ml), 54.31 ± 0.853 (100 μg/ml), 51.49 ± 1.348 (150 μg/ml), 42.6 ± 1.651 (200 μg/ml), 32.25 ± 0.688 (250 μg/ml) and 28.25 ± 0.688 for $CD44^+$ specific AGS CSCs. On the other hand the survival percent rate of OH-SWCNT in $CD44^+$cells was 81.3 ± 3.577 (50 μg/ml), 74.25 ± 0.688 (100 μg/ml), 56.225 ± 0.619 (150 μg/ml) 48.16 ± 0.44 (200 μg/ml), 38.365 ± 1.004 (250 μg/ml) and for cisplatin loaded OH-SWCNT treated $CD44^+$ cells was 78.25 ± 0.688 (50 μg/ml), 64.31 ± 0.853 (100 μg/ml), 52.49 ± 1.348 (150 μg/ml), 37.1 ± 0.275 (200 μg/ml), 28.25 ± 0.688 (250 μg/ml). All the values obtained were calculated in duplicates and are statistically significant with a $p\text{-value} < 0.001$ when determined with TWO-way ANOVA.

3.3.3. Tumorsphere inhibition assay

Tumorsphere forming assay has been used as a standard *In- vitro* method to find out sphere formation in cancer stem cells. We have used a tumorsphere inhibition assay to evaluate the potentiality of cisplatin-loaded OH-SWCNT nanocarrier in inhibiting the sphere-forming capacity of $CD133^+$ and $CD44^+$ AGS CSCs for 7 days. The results are shown in Fig. 7. The results revealed that $CD133^+$ cells that are treated with OH-SWCNT and cisplatin-loaded OH-SWCNT nanocarrier at several concentrations like 50 μg/ml,150 μg/ml, and 250 μg/ml have selectively inhibited the growth of gastric cancer stem cells subpopulation within 48 h as shown in Fig. 7(A) whereas, cisplatin loaded OH-SWCNT nanocarrier has shown stronger inhibitory effects by affecting sphere colony formation in $CD133^+$ at all concentrations (50 μg/ml, 150 μg/ml, and 250 μg/ml) when compared to OH-SWCNT. Similar results are observed in $CD44^+$ cells where the OH-SWCNT-cisp nanocarrier has a stronger inhibitory effect when compared to OH-SWCNTs at different concentrations (50 μg/ml, 150 μg/ml, and 250 μg/ml) as shown in Fig. 7(B). From our results, we also observed AGS tumrospheres when treated with cisplatin with a concentration of 250 μg/ml showed no difference when compared with control cells at day 1. On day 7 of incubation, they observed an increase in no tumrospheres stating that cisplatin showed Chemoresistance as shown in Fig. 7.

4. Discussion

Chemotherapy is a common method for the treatment of gastric cancer. The overall survival rate is only 20%. This may be due to the poor solubility of the drug and its difficulty in overcoming biological barriers and delivering a drug to the targeted site of action [3,4]. Since gastric cancer is one of the most common among chemo-sensitive malignancies at the time of initial treatment by platinum-based therapy, most patients ultimately relapse and succumb to chemo-resistant disease [40,41]. Furthermore, front-line chemotherapy is associated with toxicities and may adversely impact the quality of life [42]. Based on this scenario our goal was to first test the ability of OH-SWCNT whether it could enhance the efficacy of cisplatin and secondly to investigate its therapeutic efficiency on gastric cancer stem cells.

Several lines of evidence suggest that the heterogeneous cancer cells employ a dynamic survival strategy in which a small subpopulation assumes a reversible drug-tolerant state that can protect the population from eradication by potential lethal exposures [43]. Cancer stem cells reflect such an adaptation conferring stem-like properties to cancer cells, leading to resistance to cytotoxic drugs and metastasis. Since several studies reported that functionalized carbon nanotubes inhibited the growth of csc's population by inhibiting several signaling pathways [44,45] and also down-regulating Snail, N-Cadherin, and Vimentin both *in vitro* and *in vivo* [44], we hypothesized that OH-SWCNT can potentially act as a potent drug carrier molecule to increase the sensitivity of cells towards cisplatin.

This is probably the first report that states that OH-SWCNT nanoparticles which helps in sensitizing the gastric cancer stem cells to cisplatin by *in-vitro*. To understand the stability and therapeutic efficiency of cisplatin loaded on the surface of OH-SWCNT we have loaded different concentrations of cisplatin (50μg/ml-250 μg/ml) based on previous literature [29]. We also observed that the maximum amount of cisplatin was entrapped on OH-SWCNT at 200 μg/ml. This is possible due to the noncovalent functionalization of surfactant tween 80 and its stichometric changes during the absorption of cisplatin onto the walls of OH-SWCNT. Based on this we used 200μ/ml concentration of cisplatin-loaded OH-SWCNT for drug release kinetics study. Most interestingly our release kinetics data showed that the release of cisplatin over OH-SWCNT was performed in a controlled manner and that the release continued even after 48 h at all pHs (3.5,5.5 and 7.5). We also observed sustained release of cisplatin over OH-SWCNT is observed at acidic pHs(3.5 and 5.5) with very less difference throughout 48 h. This may be due to the physical dissociation of cisplatin from OH-SWCNT in a specific acidic pH (3.5 and 5.5) microenvironment by either hydrophobic core protonation or ionization. The half-life of cisp release from OH-SWCNT was less which suggests that it can be used for a wide range of biomedical applications by lowering possible adverse effects which can enhance their safety and stability as a targeted drug delivery molecule. Additionally, the cytocompatible studies suggest that the efficiency of cisp-loaded OH-SWCNT towards AGS cell lines showed significant cytotoxicity with $p > 0.005$. Whereas there was less or no toxicity toward HEK cell lines. The IC_{50} value of cisplatin-loaded OH-SWCNT for AGS was less than 50%, whereas the IC_{50} value for normal HEK cell lines was more than 50% showing its effulgence for controlled side effects in the case of normal cells. In this context, we confirm that our devised nanocarrier system-based drug delivery approach could potentially minimize the side effects and

Table 3
IC_{50} values of cisplatin-loaded OH-SWCNT In $CD133^{+}$ gastric cancer stem cells and $CD44^{+}$ gastric cancer stem cells. *$p < 0.001$ compared to free cisplatin.

Compound	CD133+ AGS CSC Mean ± SEM (IC50-mol/L)	$CD44^{+}$ AGS CSC Mean ± SEM (IC50-mol/L)	*P Value*
Free Cisplatin	225.675 ± 0.00882	195.64 ± 0.0196	$P < 0.001$
Cisplatin–OH–SWCNT	29.57 ± 0.0196	39.6 ± 0.0392	$P < 0.001$
Fold change in IC50	7.63 -fold decrease	4.94 -fold decrease	

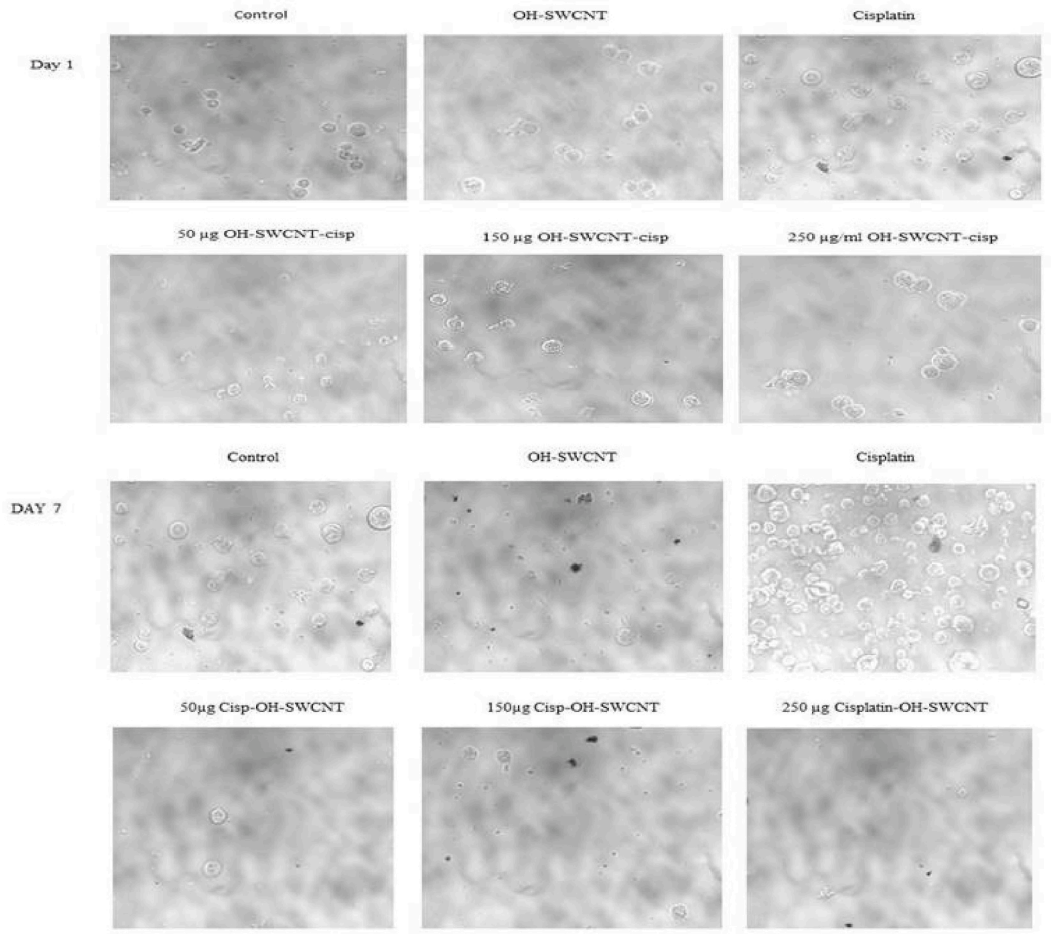

Fig. 7a. A) Effect of OH-SWCNT, Cisplatin, and Cisplatin-loaded OH-SWCNT on treatment at different concentrations (50 µg/ml, 150 µg/ml, 250 µg/ml) on sphere formation capacity and colony formation capacity on 6-well ultra-low attachment plates of $CD133^{+}$ cells *in-vitro*. Magnification: 40×.

maximize the therapeutic efficiency.

In this work, we also investigated the chemo-sensitivity of cisplatin-loaded OH-SWCNT nanocarrier system on gastric cancer stem cells to correlate the potential induction of chemoresistance of cisplatin. Our significant findings revealed that cisplatin on short-term treatment (48 h) has a critical role in causing chemoresistance over marker-specific gastric cancer stem cells (CD133+ and $CD44^{+}$). Our nanoparticle-based drug delivery system modulated it. Indeed, at a cisplatin concentration of 50 µg/ml, we observed a change in the phenotype of both CD133+ and $CD44^{+}$ specific gastric cancer stem cells with a decrease in their survival percent. Based on the promising results obtained in this study it can be concluded that the cisplatin-loaded OH-SWCNT nanocarrier could be a suitable nanocarrier system for eradicating gastric cancer stem cells population.

5. Conclusion

The cisplatin-loaded hydroxyl functionalized single-walled carbon nanotube-based nanocarrier was efficient in targeting CSCs

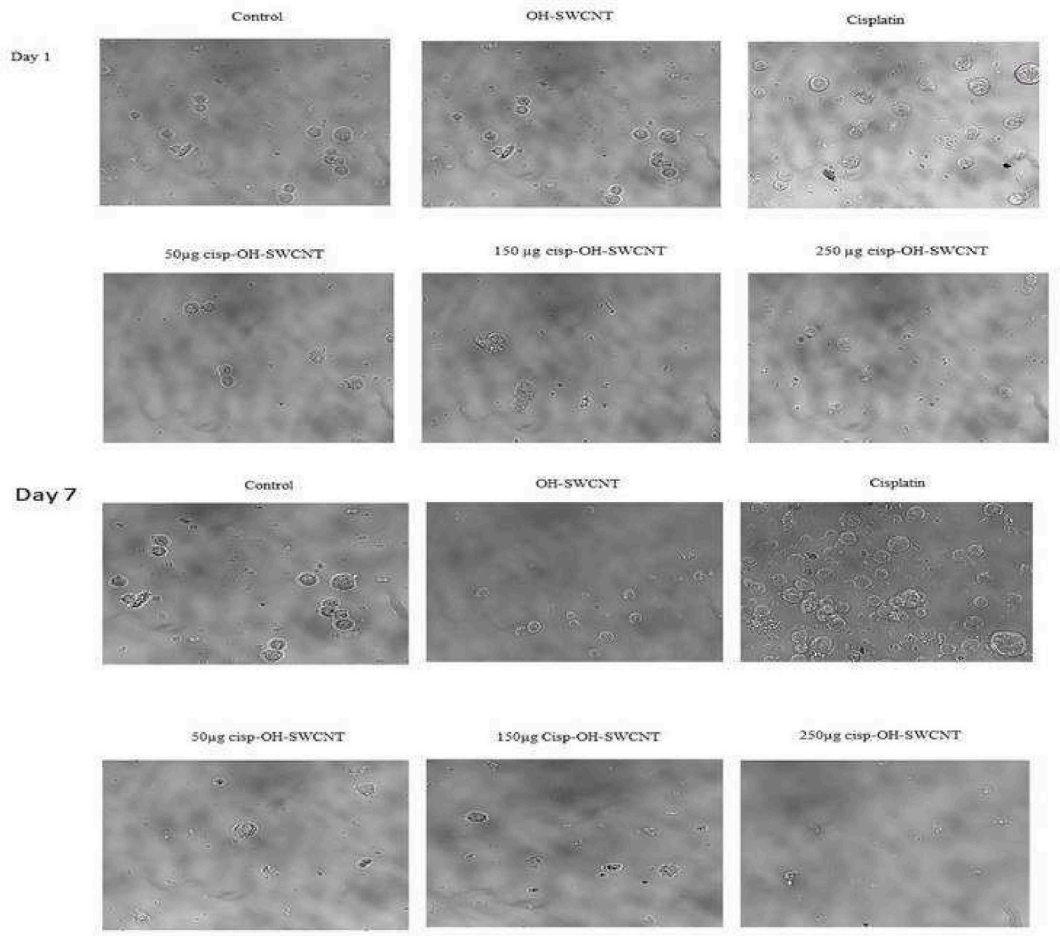

Fig. 7b. B): Effect of OH-SWCNT, Cisplatin, and cisplatin-loaded OH-SWCNT on treatment at different concentrations (50 µg/ml, 150 µg/ml, 250 µg/ml) on sphere formation capacity and colony formation capacity on 6-well ultra-low attachment plates of $CD44^{+}$ cells *in-vitro*. Magnification: 40×.

growth when compared to OH-SWCNT and cisp. It was observed that there was a long-term release of cisplatin over OH-SWCNT throughout 48 h at pHs 3.5 and 5.5 when compared to release at pH7.4 showing that OH-SWCNT is an effective drug delivery vehicle for sustained and controlled release of drug to targeted site of action. UV–visible, FT-IR, and HR-TEM were used to conform non-covalent interaction of cisplatin on the surface of OH-SWCNT. The cytotoxicity data showed a significant *P-value* ($p > 0.005$) with cisplatin-loaded OH-SWCNT incubated cells. Furthermore, cisplatin-loaded OH-SWCNT nanocarrier showed stronger inhibition ability of both proliferation assay and tumorsphere formation assay in both $CD133^{+}$ and $CD44^{+}$ CSCs. In conclusion to the results obtained OH-SWCNT nanoparticle encapsulation alters the bioavailability properties of cisplatin, influencing its pharmacodynamic performance at the cellular level and potentially affecting the growth of cancer stem cells. The current study could be a starting point for developing an effective strategy for treating gastric CSCs, with the potential to improve gastric cancer therapy.

Credit to author contribution statement

Conceived and designed the experiments- A.N.K.V Sravani, N.Chandrasekaran, John Thomas, Amitava Mukherjee.
Performed the experiments- AN.K.V Sravani, N.Chandrasekaran.
Analyzed and interpreted the data- A.N.K.V Sravani, N.Chandrasekaran, John Thomas, Amitava Mukherjee.
Contributed reagents, materials, analysis tools or data- A.N.K.V Sravani, N.Chandrasekaran, John Thomas, Amitava Mukherjee.
Wrote the paper- A.N.K.V Sravani, N.Chandrasekaran, John Thomas, Amitava Mukherjee.

Funding

"The research received no external funding".

Declaration of competing interest

The authors involved reveal no sources of conflict of interest.

Acknowledgments

The authors are thankful to the Vellore Institute of Technology for providing the lab facilities to carry out the research work.

References

[1] H. Juan Yao, Y. ge Zhang, L. Sun, Y. Liu, The effect of hyaluronic acid functionalized carbon nanotubes loaded with salinomycin on gastric cancer stem cells, Biomaterials 35 (33) (2014) 9208–9223, https://doi.org/10.1016/j.biomaterials.2014.07.033.
[2] A. Jemal, F. Bray, J. Ferlay, Global cancer statistics: 2011, 1,33-64, Ca - Cancer J. Clin. 49 (2) (1999), https://doi.org/10.3322/caac.20107.Available.
[3] E. Heister, V. Neves, C. Tîlmaciu, K. Lipert, V.S. Beltrán, H.M. Coley, S.R.P. Silva, J. McFadden, Triple functionalisation of single-walled carbon nanotubes with doxorubicin, a monoclonal antibody, and a fluorescent marker for targeted cancer therapy, Carbon N. Y. 47 (9) (2009) 2152–2160, https://doi.org/10.1016/j.carbon.2009.03.057.
[4] E. Blanco, H. Shen, M. Ferrari, Principles of nanoparticle design for overcoming biological barriers to drug delivery, Nat. Biotechnol. 33 (9) (2015) 941–951, https://doi.org/10.1038/nbt.3330.
[5] A.Z. Ayob, T.S. Ramasamy, Cancer stem cells as key drivers of tumour progression, J. Biomed. Sci. 25 (1) (2018) 1–18, https://doi.org/10.1186/s12929-018-0426-4.
[6] B. Beck, C. Blanpain, Unravelling cancer stem cell potential, Nat. Rev. Cancer 13 (10) (2013) 727–738, https://doi.org/10.1038/nrc3597.
[7] J.C. Chang, Cancer stem cells: role in tumor growth, recurrence, metastasis, and treatment resistance, Med. (United States) 95 (1) (2016) S20–S25, https://doi.org/10.1097/MD.0000000000004766.
[8] J.A. Ajani, S. Song, H.S. Hochster, I.B. Steinberg, Cancer stem cells: the promise and the potential, Semin. Oncol. 42 (S1) (2015), https://doi.org/10.1053/j.seminoncol.2015.01.001. S3–S17.
[9] K. Chen, Y.H. Huang, J.L. Chen, Understanding and targeting cancer stem cells: therapeutic implications and challenges, Acta Pharmacol. Sin. 34 (6) (2013) 732–740, https://doi.org/10.1038/aps.2013.27.
[10] M. Prieto-Vila, R.U. Takahashi, W. Usuba, I. Kohama, T. Ochiya, Drug resistance driven by cancer stem cells and their niche, Int. J. Mol. Sci. 18 (12) (2017), https://doi.org/10.3390/ijms18122574.
[11] H. Chen, J. Lin, Y. Shan, L. Zhengmao, The promotion of nanoparticle delivery to two populations of gastric cancer stem cells by CD133 and CD44 antibodies, Biomed. Pharmacother. 115 (February) (2019), https://doi.org/10.1016/j.biopha.2019.108857.
[12] X. Zhang, R. Hua, X. Wang, M. Huang, L. Gan, Z. Wu, J. Zhang, H. Wang, Y. Cheng, J. Li, W. Guo, Identification of stem-like cells and clinical significance of candidate stem cell markers in gastric cancer, Oncotarget 7 (9) (2016) 9815–9831, https://doi.org/10.18632/oncotarget.6890.
[13] P. Xia, X.Y. Xu, DKK3 attenuates the cytotoxic effect of natural killer cells on CD133+ gastric cancer cells, Mol. Carcinog. 56 (7) (2017) 1712–1721, https://doi.org/10.1002/mc.22628.
[14] S. Takaishi, T. Okumura, S. Tu, S.S.W. Wang, W. Shibata, R. Vigneshwaran, S.A.K. Gordon, Y. Shimada, T.C. Wang, Identification of gastric cancer stem cells using the cell surface marker CD44, Stem Cell. 27 (5) (2009) 1006–1020, https://doi.org/10.1002/stem.30.
[15] S.R. Singh, Gastric cancer stem cells: a novel therapeutic target, Cancer Lett. 338 (1) (2013) 110–119, https://doi.org/10.1016/j.canlet.2013.03.035.
[16] F. Yang, Z. Zheng, L. Zheng, J. Qin, H. Li, X. Xue, J. Gao, G. Fang, SATB1 SiRNA-encapsulated immunoliposomes conjugated with CD44 antibodies target and eliminate gastric cancer-initiating cells, OncoTargets Ther. 11 (2018) 6811–6825, https://doi.org/10.2147/OTT.S182437.
[17] J.E. Visvader, G.J. Lindeman, Cancer stem cells: current status and evolving complexities, Cell Stem Cell 10 (6) (2012) 717–728, https://doi.org/10.1016/j.stem.2012.05.007.
[18] H. Song, X. Su, K. Yang, F. Niu, J. Li, J. Song, H. Chen, B. Li, W. Li, W. Qian, X. Cao, S. Guo, J. Dai, S.S. Feng, Y. Guo, C. Yin, J. Gao, CD20 antibody-conjugated immunoliposomes for targeted chemotherapy of melanoma cancer initiating cells, J. Biomed. Nanotechnol. 11 (11) (2015) 1927–1946, https://doi.org/10.1166/jbn.2015.2129.
[19] R. Dubey, D. Dutta, A. Sarkar, P. Chattopadhyay, Functionalized carbon nanotubes: synthesis, properties and applications in water purification, drug delivery, and material and biomedical sciences, Nanoscale Adv. 3 (20) (2021) 5722–5744, https://doi.org/10.1039/d1na00293g.
[20] A. Venkataraman, E.V. Amadi, Y. Chen, C. Papadopoulos, Carbon nanotube assembly and integration for applications, Nanoscale Res. Lett. 14 (1) (2019), https://doi.org/10.1186/s11671-019-3046-3.
[21] W. Zhang, Z. Zhang, Y. Zhang, The application of carbon nanotubes in target drug delivery systems for cancer therapies, Nanoscale Res. Lett. 6 (2011) 1–22, https://doi.org/10.1186/1556-276X-6-555.
[22] N. Sohrabi, A. Alihosseini, V. Pirouzfar, M.Z. Pedram, Analysis of dynamics targeting CNT-based drug delivery through lung cancer cells: design, simulation, and computational approach, Membranes 10 (10) (2020) 1–16, https://doi.org/10.3390/membranes10100283.
[23] J.M. Tan, P. Arulselvan, S. Fakurazi, H. Ithnin, M.Z. Hussein, A review on characterizations and biocompatibility of functionalized carbon nanotubes in drug delivery design, J. Nanomater. 2014 (1) (2014), https://doi.org/10.1155/2014/917024.
[24] M. Nicoletti, C. Gambarotti, E. Fasoli, Proteomic exploration of soft and hard biocorona onto PEGylated multiwalled carbon nanotubes, Biotechnol. Appl. Biochem. 68 (5) (2021) 1003–1013, https://doi.org/10.1002/bab.2020.
[25] A. Brown, S. Kumar, P.B. Tchounwou, Cisplatin-based chemotherapy of human cancers, J. Cancer Sci. Ther. 11 (4) (2019).
[26] S. Dasari, P. Bernard Tchounwou, Cisplatin in cancer therapy: molecular mechanisms of action, Eur. J. Pharmacol. 740 (2014) 364–378, https://doi.org/10.1016/j.ejphar.2014.07.025.
[27] L. Wang, X. Zhao, J. Fu, W. Xu, J. Yuan, The role of tumour metabolism in cisplatin resistance, Front. Mol. Biosci. 8 (June) (2021) 1–13, https://doi.org/10.3389/fmolb.2021.691795.
[28] G. Sekar, A. Mukherjee, N. Chandrasekaran, Comprehensive spectroscopic studies on the interaction of biomolecules with surfactant detached multi-walled carbon nanotubes, Colloids Surf. B Biointerfaces 128 (2015) 315–321, https://doi.org/10.1016/j.colsurfb.2015.02.006.
[29] M. Magid, L.Q. Al-Karam, Non-covalent functionalization of CNTs with chitosan for drug delivery system, J. Phys. Conf. Ser 2114 (1) (2021), https://doi.org/10.1088/1742-6596/2114/1/012038.
[30] S. Yang, Z. Wang, Y. Ping, Y. Miao, Y. Xiao, L. Qu, L. Zhang, Y. Hu, J. Wang, PEG/PEI-Functionalized single-walled carbon nanotubes as delivery carriers for doxorubicin: synthesis, characterization, and in vitro evaluation, Beilstein J. Nanotechnol. 11 (2020) 1728–1741, https://doi.org/10.3762/BJNANO.11.155.
[31] W.A. Al-Otaibi, M.H. Alkhatib, A.N. Wali, Cytotoxicity and apoptosis enhancement in breast and cervical cancer cells upon coadministration of mitomycin C and essential oils in nanoemulsion formulations, Biomed. Pharmacother. 106 (May) (2018) 946–955, https://doi.org/10.1016/j.biopha.2018.07.041.
[32] T. Borjigin, G. Zhao, Y. Zhang, M. Liang, B. Liu, H. Liu, X. Yang, H. Guo, Control loading Au nanoparticles on the surface of hydroxyl pillar[5]Arene functionalized single-walled carbon nanotubes and its application in catalysis and sensing, Sustain. Energy Fuels 3 (9) (2019) 2312–2320, https://doi.org/10.1039/c9se00290a.
[33] H. Kato, K. Mizuno, M. Shimada, A. Nakamura, K. Takahashi, K. Hata, S. Kinugasa, Observations of bound Tween80 surfactant molecules on single-walled carbon nanotubes in an aqueous solution, Carbon N. Y. 47 (15) (2009) 3434–3440, https://doi.org/10.1016/j.carbon.2009.08.006.

[34] Z. Marković, S. Jovanović, D. Kleut, N. Romčević, V. Jokanović, V. Trajković, B. Todorović-Marković, Comparative study on modification of single wall carbon nanotubes by sodium dodecylbenzene sulfonate and melamine sulfonate superplasticiser, Appl. Surf. Sci. 255 (12) (2009) 6359–6366.
[35] M.A. Badea, M. Prodana, A. Dinischiotu, C. Crihana, D. Ionita, M. Balas, Cisplatin loaded multiwalled carbon nanotubes induce resistance in triple negative breast cancer cells, Pharmaceutics 10 (4) (2018), https://doi.org/10.3390/pharmaceutics10040228.
[36] S. Senapati, A.K. Mahanta, S. Kumar, P. Maiti, Controlled drug delivery vehicles for cancer treatment and their performance, Signal Transduct. Targeted Ther. 3 (1) (2018) 1–19, https://doi.org/10.1038/s41392-017-0004-3.
[37] M. Sun, W. Zhou, Y.Y. Zhang, D.L. Wang, X.L. Wu, CD44+ gastric cancer cells with stemness properties are chemoradioresistant and highly invasive, Oncol. Lett. 5 (6) (2013) 1793–1798, https://doi.org/10.3892/ol.2013.1272.
[38] O.O. Ogbole, P.A. Segun, A.J. Adeniji, In Vitro Cytotoxic Activity of Medicinal Plants from Nigeria Ethnomedicine on Rhabdomyosarcoma Cancer Cell Line and HPLC Analysis of Active Extracts, 2017, pp. 1–10, https://doi.org/10.1186/s12906-017-2005-8.
[39] T. Chen, K. Yang, J. Yu, W. Meng, D. Yuan, F. Bi, F. Liu, J. Liu, B. Dai, X. Chen, F. Wang, F. Zeng, H. Xu, J. Hu, X. Mo, Identification and expansion of cancer stem cells in tumor tissues and peripheral blood-derived from gastric adenocarcinoma patients, Cell Res. 22 (1) (2012) 248–258, https://doi.org/10.1038/cr.2011.109.
[40] T. Van Nyen, M. Planque, L. van Wagensveld, J.A.G. Duarte, E.A. Zaal, A. Talebi, M. Rossi, P.R. Körner, L. Rizzotto, S. Moens, W. De Wispelaere, R.E.M. Baiden-Amissah, G.S. Sonke, H.M. Horlings, G. Eelen, E. Berardi, J.V. Swinnen, C.R. Berkers, P. Carmeliet, D. Lambrechts, B. Davidson, R. Agami, S.M. Fendt, D. Annibali, F. Amant, Serine metabolism remodeling after platinum-based chemotherapy identifies vulnerabilities in a subgroup of resistant ovarian cancers, Nat. Commun. 13 (1) (2022), https://doi.org/10.1038/s41467-022-32272-6.
[41] D.W. Shen, L.M. Pouliot, M.D. Hall, M.M. Gottesman, Cisplatin resistance: a cellular self-defense mechanism resulting from multiple epigenetic and genetic changes, Pharmacol. Rev. 64 (3) (2012) 706–721, https://doi.org/10.1124/pr.111.005637.
[42] B. Bortot, M. Mongiat, E. Valencic, S. Dal Monego, D. Licastro, M. Crosera, G. Adami, E. Rampazzo, G. Ricci, F. Romano, G.M. Severini, S. Biffi, Nanotechnology-based cisplatin intracellular delivery to enhance chemo-sensitivity of ovarian cancer, Int. J. Nanomed. 15 (2020) 4793–4810, https://doi.org/10.2147/IJN.S247114.
[43] S.V. Sharma, D.Y. Lee, B. Li, M.P. Quinlan, S. Maheswaran, U. Mcdermott, N. Azizian, L. Zou, M.A. Fischbach, K. Wong, K. Brandstetter, B. Wittner, M. Classon, J. Settleman, NIH Public Access 141 (1) (2011) 69–80, https://doi.org/10.1016/j.cell.2010.02.027.A.
[44] L. Tang, Q. Xiao, Y. Mei, S. He, Z. Zhang, R. Wang, W. Wang, Insights on functionalized carbon nanotubes for cancer theranostics, J. Nanobiotechnol. 19 (1) (2021) 1–28, https://doi.org/10.1186/s12951-021-01174-y.
[45] M.A. Badea, M. Balas, M. Prodana, F.G. Cojocaru, D. Ionita, A. Dinischiotu, Carboxyl-functionalized carbon nanotubes loaded with cisplatin promote the inhibition of PI3K/akt pathway and suppress the migration of breast cancer cells, Pharmaceutics 14 (2) (2022), https://doi.org/10.3390/pharmaceutics14020469.